JOURNAL OF Applied Polymer SCIENCE

Fabrication and Characterization of HCl-Treated Clinoptilolite Filled Ethylene Vinyl Acetate Composite Films

Ajay K. Mishra, Shivani B. Mishra, Bhekie B. Mamba, Derrick S. Dlamini, Thabo S. Mthombo
Department of Applied chemistry, University of Johannesburg, Doornfontein 2028, Johannesburg, South Africa
Correspondence to: A. K. Mishra (E-mail: amishra@uj.ac.za)

ABSTRACT: As received and HCl treated Clinoptilolite (C)-ethylene vinyl acetate (EVA) composites were prepared via the melt-mixing technique, and extruded through a single-screw extruder to obtain composite strips with an average thickness of 0.5 mm. The films were then characterized for their morphological, structural, thermal, and mechanical properties. Optical micrographs show that at higher C loading, the particles form large agglomerates, resulting in the formation of voids on the surface of the films. With increasing zeolite loading, the films become brittle, resulting in reduced Young's modulus. Acid treatment of the C tends to affect the crystal structure of the zeolite, resulting in poor tensile properties of the HCl-treated zeolite-filled EVA films. Addition of the zeolite also increased the crystallinity of the structure, acting as a nucleating agent in the EVA crystallization. Modeling of the tensile yield data with Pukanszky model indicate that there is poor interfacial adhesion between the polymer matrix and the filler particles. Thermal characterization studies showed that addition of the zeolites retarded the onset degradation temperature of EVA. However, degradation temperatures including T_{max} and the final decomposed temperature were increased, suggesting improved thermal stability due to reduced inter-chain mobility in the composite materials as a result of increased zeolite loading. © 2012 Wiley Periodicals, Inc. J. Appl. Polym. Sci. 000: 000–000, 2012

KEYWORDS: clinoptilolite; EVA; melt-mixing; composites; tensile and mechanical

Received 8 September 2011; accepted 25 April 2012; published online 00 Month 2012
DOI: 10.1002/app.38021

INTRODUCTION

In recent decades, research has been focused on the production of polymeric materials, with the ultimate goal of producing materials with enhanced performance. Particulate-filled polymer composites have been used in fields such as drug-delivery systems, food packaging, automobile, and protective coating industries.[1,2] Polymer composites are normally obtained in one of the two methods: the most popular is to introduce nanoscale particles into a polymer matrix to produce polymer/nanoparticle composites, while the other entails the fabrication of the polymer materials themselves on the nanoscale.[3] In the former case, incorporation of the particles into the polymer matrix can be achieved by using one of the two following approaches: (i) by insertion of suitable monomers into the silicate galleries of the filler, followed by subsequent polymerization or (ii) by direct insertion of the polymer chains into the silicate galleries in the molten state.[4]

Recently, the method of melt intercalation has been the most preferred in the preparation of particulate-filed polymer composites. Melt intercalation is achieved in melt-blending technique. The melt-blending method involves the physical mixing of the polymer matrix and the filer in the molten state of the polymer. One advantage of this approach is that no organic solvent is used thereby minimizing environmental concerns, and it is compatible with industrial polymer extrusion and blending processes. The physical mixing of a polymer and a filler (i.e., clay) results in composites with either exfoliated or interacted structures, sometimes both, depending on the degree of penetration of the polymer into the layered silicate galleries of the filler.[5] Nanofillers such as clays, silver, calcium carbonate, and talc have been widely used, and recently, different types of zeolitic materials have also been employed as particulate fillers into the polymer matrices.[6]

Zeolites are naturally occurring crystalline aluminosilicates consisting of a framework of tetrahedral molecules linked to each other by corner-sharing oxygen atoms. Isomorphic substitution of, for example, Al^{3+} for Si^{4+} within the framework generates negative charges that are counterbalanced by alkali or alkaline cations situated in the interlayer. These cations are coordinated with a defined number of water molecules, and are bound to the aluminosilicate framework by weaker electrostatic bonds, allowing the intercalation of small particles in between the particles to occur.[7,8]

Although an extensive amount of research work has been done in the fields of polymer-based composites, most of the studies were conducted with calcium carbonate, silver nanoparticles, and clay, and very few studies have been reported with zeolites as the filler material.[1,6] Amongst all the potential nanocomposite precursors, zeolites have attracted more interest, probably because they are readily available at low cost, and no toxicity effects have been reported. Zeolites with polymers composites results in an improved mechanical, thermal, and physicochemical property when compared with the original polymer.

Composites have found a potential application in water treatment.[9–11] Most adsorbents have been used in a powder form and there has been a challenge of complete recovery. Recently, polymers have been used as a support for known adsorbents to improve recovery after adsorption and for convenient handling. As mentioned earlier, the melt-blending method of composite synthesis is superb for this purpose. This method use thermoplastic polymers like ethylene vinyl acetate (EVA). Even though most thermoplastics are hydrophobic, they are good in fabricating an adsorbent that will be stable in aquatic environments. Now, since clinoptilolite (C) (filler) is hydrophilic and the EVA (matrix) used in this work was relatively hydrophobic, the filler was treated with HCl, to improved crosslinking. It is widely accepted that zeolites treated with an acid bond well with hydrophobic polymers while base-treated zeolites adhere well on hydrophilic polymers. The downside with impregnating a known adsorbent into a less hydrophilic polymer like EVA is that a lot of the powder (filler) is used than when it is used in adsorption in the powder form to make sure that more adsorption sites are on the surface of the polymer. Treating zeolites with HCl is also good in improving surface area.

The results of this work are presented in a series of two papers. The first paper, published separately, focus on the applicability of the composites in heavy metal removal.[11] In that study, we investigated the effect of sorbent dose (5–30 wt %) on the percentage removal of Pb^{2+}, Cu^{2+}, and Co^{2+} ions. For all these metal ions, the removal efficiency increased with an increase in the amount of C in the composite. The effect of contact time on the metal-ion retention capacity was also investigated by varying the time from 0 to 48 h, at a fixed initial concentration of 10 mgL^{-1}. The trend in the change in adsorption efficiency with contact time was the same. The adsorption increased over time, and equilibrium was reached after 24 h. To investigate the influence of pretreatment, composites filled with "as-received" C were compared with composites filled with NaCl-, HCl-, and KCl-treated C particles.

Herein, the preparation and characterization of HCl-treated C-EVA and C-EVA composites is reported. EVA, although non-biodegradable, is a relatively hydrophilic polymer with excellent cohesive strength and film-forming properties. The effects of filler loading into the polymer matrix and the pretreatment of the zeolite on the thermal, mechanical, and structural properties of the composites were investigated. The results presented in this article may improve our understanding of the intrinsic structure of zeolite-EVA composite materials, and thus help composite material scientists identify opportunities for further improvement and optimization of composite synthesis.

EXPERIMENTAL

Materials

The C, as received zeolite, used in this study was supplied by Pratley South Africa and was sourced from the Vulture Creek in the KwaZulu-Natal Province of South Africa. EVA (with 10% vinyl acetate) is a commercial product bought from Plastamid, South Africa. For acid treatment of the zeolite, 32% HCl was used as the conditioning reagent. The reagent was of the highest quality, and was supplied by Sigma Aldrich, South Africa.

Preparation of Filler Material

As received sample of the zeolite were grounded and washed with deionized water before being oven dried at 105°C overnight. The dried particles were then screened through a 38 μm sieve. It should be mentioned that the zeolites were treated under uncontrolled conditions because, as highlighted in the introduction, the purpose of fabricating the C-EVA composites was to use it for heavy metal adsorption. For that reason, the loss of crystallinity on the zeolites was permitted because crystalline materials are not good water absorbents. The treatment of the filler was done as follows: A portion of the <38 μm particles were subjected to HCl treatment. A 2*M* solutions of HCl were used as the conditioning media. Zeolites particles were soaked in 100 mL of the acid solution in a 250-mL volumetric flask and stirred for 24 h at 160 rpm at room temperature. In all the experiments, the solid to liquid ratio was kept constant as 10 : 100 (w/v). The slurry was then filtrated via a 0.5-mm filter paper and washed three times with deionized water to remove excessive anions.

Fabrication of Composites

All C-EVA composites were prepared by the melt-mixing technique in a rheomixer (Haake Rheomex OS) at 120°C and at a speed of 60 rpm for 30 min. The mass of polymer or filler required for specific ratios from 100 : 0 to 70 : 30 (polymer/zeolite) was calculated using the "mixing" equation below:

$$m = \rho \times V_c \times f_r \times W_t \quad (1)$$

where: m is the mass (g), ρ is the density of polymer (or C), V_c and f_r are constants for the chamber volume and filler rate of the rheomixer, respectively, W_t (%) represents the required weight of polymer or filler.

The composite strips were then extruded through a single-screw extruder at 120°C, to obtain strips from a 50 mm by 0.5 mm sheet die.

Characterization of Filler and Composites

X-ray Fluorescence Spectroscopy. The elemental composition of the as received and HCl-treated zeolites was determined by X-ray fluorescence (XRF) performed by Philips Magix Pro XRF spectrometer connected to a computer operated with SuperQ Manager Software.

Scanning Electron Microscopy. The morphology and dispersion of the filler in the polymer matrix were examined with a JOEL scanning electron microscopy (SEM) 5600 with a field-

emission gun operating under the following conditions: 15 kV acceleration voltage, working distance (WD) of 20, and spot size of 21. Specimens were deposited on double-sided carbon conductive scotch tape and examined on the surface after double coating with carbon for charge accumulation.

Fourier Transform Infrared Spectroscopy. A Bruker Tensor 27 Fourier transform infrared (FTIR) spectrometer was used to examine the structural aspects of the composites. The data were analyzed with OPUS software. This FTIR model uses a diamond/ZnSe universal ATR. Therefore, a small sample was sliced from the polymeric composites and characterized at room temperature.

X-ray Diffraction Analysis. X-ray diffraction analysis (XRD) data of the composites were collected using a Philips Panalytical X'pert Diffractometer with 40 mA, 40 keV, Cu Kα radiation ($\lambda = 0.1540562$ nm), divergence slit 1/8°, anti-scatter slits 1/4°, 5mm, and a range of 4–60° on the 2θ scale.

Brunuer–Emmett–Teller analysis. Surface analysis was done using the Brunuer–Emmett–Teller (BET) method with an automated gas adsorption analyser (Micromeritics ASAP 2020). Samples, prior to analyses were first degassed (cleaned) under nitrogen atmosphere for 6 h at 150°C at a N_2 flow rate of 60 mL/min.

Thermogravimetric Analysis. Thermogravimetric analysis on the fabricated composites was performed with a Perkin Elmer TGA 4000 Analyser equipped with Pyris software; sample mass, 6–10 mg; temperature range, 25–900°C; heating rate, 10°C/min. The analyses were performed in air (purged in nitrogen) at a flow rate of 80 mL/min.

Tensile Tests. Tensile (mechanical) tests of the extruded strips of an average width of 0.5 mm were carried out on an Instron machine (Instron 4443). All samples were first kept at below 50% humidity for 48 h, and then cut into "test specimen." The tests were carried out at crosshead speed of 50 mm/min at room temperature. Five trials were performed for each sample, and the mean values were used.

RESULTS AND DISCUSSION

Characterization of the Filler Material

The as received zeolite comprised 12.42% Al_2O_3, 71.37% SiO_2, 3.77% K_2O, 1.31% Na_2O, 1.29% CaO, as well as TiO_2 and Fe_2O_3 in trace quantities. From this XRF data, the Si/Al ratio was calculated to be 5.7, which is within the acceptable range characteristic of C.[12] From the BET analysis, a slight increase from 15.96 m^2/g to 20.24 m^2/g was observed in the surface area of the zeolite as a result of acid conditioning.

Untreated and HCl-treated samples of the South African zeolite were also characterized with FTIR, and the spectra are shown in Figure 1. The stretching bands shown between 1500 cm^{-1} and 1000 cm^{-1} are characteristic of zeolitic minerals. The strong IR band at 1001 cm^{-1} is characteristic of all forms of C, and is representative of the Si—O stretching. Evidently, after acid treatment the Si—O band decreased probably because of chemical interaction between the HCl and the zeolites. The peak at 1636 cm^{-1} indicates the presence of molecular water in the C sample.[13]

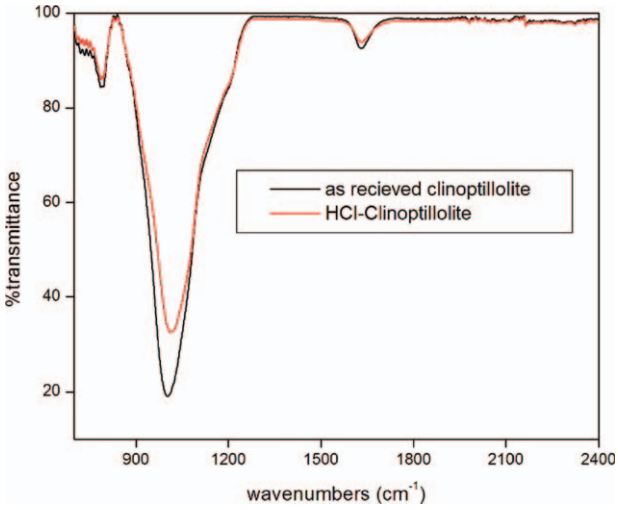

Figure 1. FTIR spectra of as received and HCl-treated zeolite. [Color figure can be viewed in the online issue, which is available at wileyonlinelibrary.com.]

Morphological Properties of the C-EVA Films

To ascertain the effect of pre-treatment on the surface morphology of the zeolite, samples were observed under SEM, and the micrographs are shown in Figure 2. At low magnification, the C particles are irregularly shaped with no visible difference between the original and chemically conditioned forms of the zeolite. However, a significant change in the morphology is observed between the as received and the HCl-treated C at higher magnification. It is evident that conditioning tends to soften and open up the surface yielding some "flake-like" structures for HCl-treated samples, as compared to the "rough and compact" structure of the original form. This could be due to the dissolution and decatination of amorphous silica fragments by the acid.[14]

The surface morphology of the plain polymer and that of the C-EVA composites with varying C loadings is shown in Figure 3. The microstructure of the plain EVA film is shown in Figure 3(a), from which the uniform orientation of the EVA molecules can be observed. The effect of zeolite loading on the polymer matrix was also examined. Figure 3(b, c) shows the typical scanning electron micrographs of C-EVA films filled with 5 and 30% of the filler, respectively. Although the particles were sieved through a 38-μm sieve, agglomerates of the zeolite particles (spherical white particles) were visible within the EVA matrix, perhaps due to interface incompatibility between the matrix and the filler phases, leading to a non-uniform distribution of the filler on the composite films. These agglomerates then result in the formation of voids, particularly around the zeolite particles, as seen in Figure 3(c).

Powder diffraction measurements of the as received zeolite confirmed C as the main component with characteristic peaks observed at $2\theta = 10.4°$ and 23.4°. Also present in trace quantities were quartz and sadinine. For comparison, the XRD patterns of the composites filled with 10, 15, and 30% of the untreated zeolites are also shown in Figure 4. It can also be observed that with increasing C loading in the composite, the spacing at the base of the peaks slightly increases, resulting in a

Applied Polymer SCIENCE

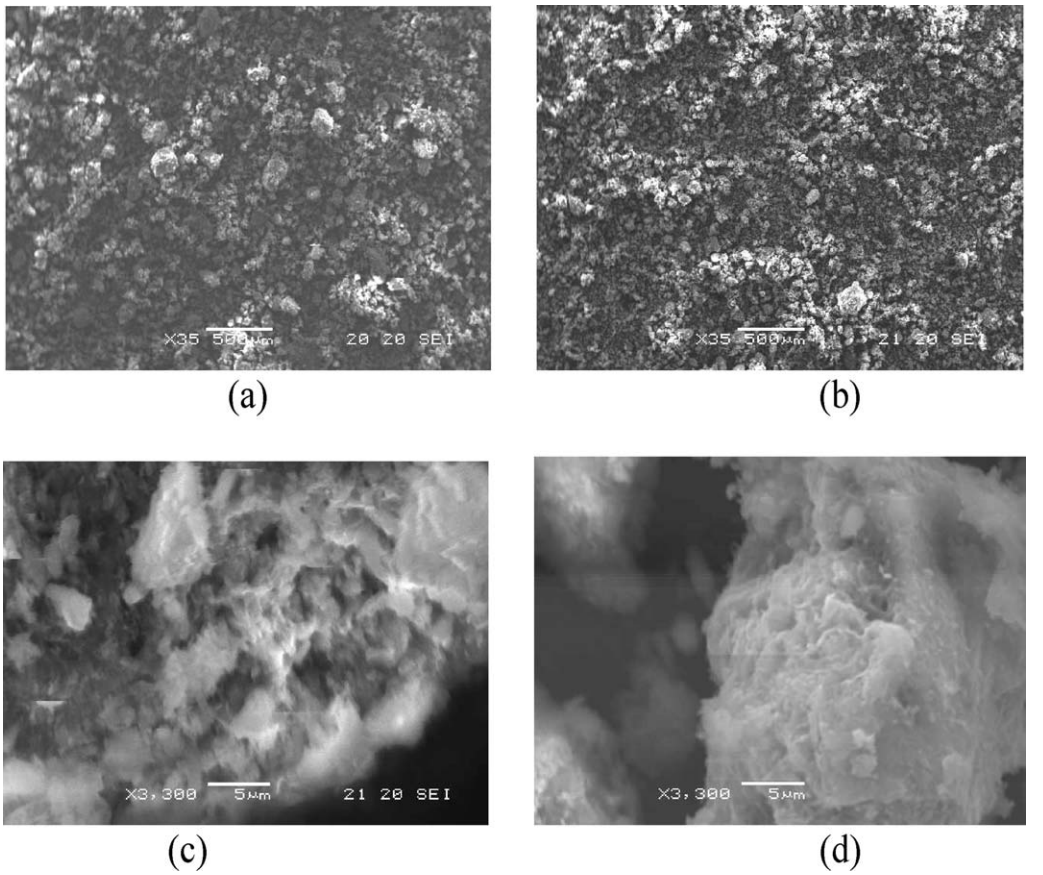

Figure 2. SEM micrographs of as received and HCl-treated C particles at: (a) and (c) low magnification (35×); (b) and (d) higher magnification (3300×).

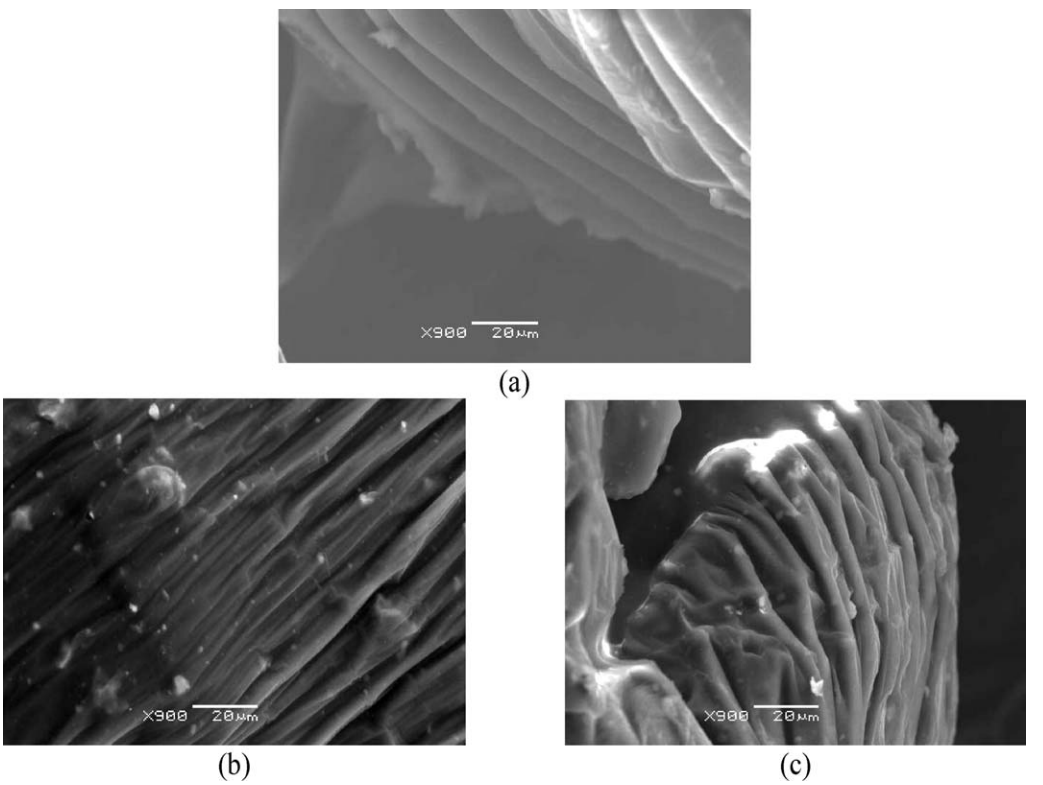

Figure 3. Surface morphology of (a) plain EVA, (b) C-EVA filled with 5% as received C, and 30% in (c).

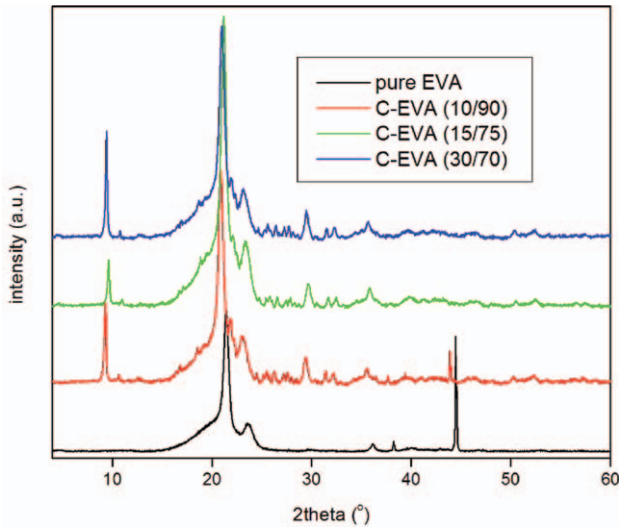

Figure 4. X-ray diffraction patterns of C-EVA composites filled with 10%, 15%, and 30% of the untreated filler. For comparison, the XRD pattern of the original C is also included. [Color figure can be viewed in the online issue, which is available at wileyonlinelibrary.com.]

shift of the peaks to lower 2θ values, suggesting that the ordered framework of the zeolite is disrupted due to intercalation with the polymer.[15] This intercalation could be largely enhanced by the strong dipole–dipole interaction between the carboxylic groups of the EVA copolymer and the silica-oxygen layers existing on the zeolite framework.[16] The presence of characteristic peaks of the zeolite in the C-EVA composites suggests that C partially keeps its original crystal structure, and exists as primary particles. The XRD of the C-EVA materials is summarized in Table I. Crystallographic spacing and crystalline size was calculated using Bragg's [eq. (2)] and Scherrer's [eq. (3)] equation,[17] respectively, as described below:

$$\lambda = 2d \sin\theta \tag{2}$$

$$\Gamma = \frac{\lambda K}{\beta \cos\theta} \tag{3}$$

where: λ is the X-ray wavelength, θ is Bragg's angle and d is the distance between atomic layers in a crystal, Γ represents the mean size of the ordered domains, K is the shape factor, and β is the line broadening at half maximum intensity (FWHM).

The % crystallinity was calculated from the ratio of the crystallinity of the composite material to that of the 100% crystalline material. From the data in Table I, it can be observed that the d-spacing increases with an increase in zeolite content in the composite material, resulting in a decrease in the 2θ values. Addition of the zeolite also increased the crystallinity of the structure, acting as a nucleating agent in the EVA crystallization. The XRD results of the HCl-C-EVA and C-EVA with 5% filler content are compared in Figure 5. The EVA crystalline peak (at 21°) increased after adding the acid-treated zeolites.

Mechanical Properties

The tensile properties of the extruded films and the plain EVA (control) are summarized in Table II. The results show that addition of the zeolite onto the polymer matrix increases the Young's modulus initially, but decreases at higher percentage weight (30%) of the filler. This decrease could be attributed to the formation of voids around the filler agglomerates at higher filler dose due to poor interfacial interaction between the polymer matrix and the filler. A decrease was also observed in the stress at break and elongation at break of the composite strips with increasing zeolite dose. The 30% zeolite containing films had the lowest stress at break (6.2 MPa) compared to the control (11.4 MPa) while the elongation at break decreased by 108.6% from the initial 453.1% of the plain polymer, as seen in Table II. The low elongation at break values indicates the presence of the brittle fracture of the films.

The Young's modulus of the HCl-C-EVA composite films at different zeolite loading was found to be as follows: 420.7 MPa (0/100), 148.4 (5/95), 159.4 MPa (10/90), 170.5 MPa (15/85), 184.8 MPa (20/80), and 202.4 MPa (30/70). A significant decrease in the Young's modulus could be attributed to the action of the acid on the filler. It has been reported that acid treatment of C results in the decatination, dealumination, and dissolution of amorphous silica fragments within the framework.[18–20] A study by Korkuna et al revealed that there was a change in the microstructure of the C as a result of dilute acid treatment.[21] It is this effect on the structure that could perhaps result in the poor mechanical strength of the zeolite hence a decrease in the Young's modulus of the C-EVA films filled with acid-treated C.

One of the most fundamental factors affecting the mechanical properties of composites is the interfacial compatibility of the polymer matrix with the filler material. To investigate the effect of interfacial interaction, the experimental tensile data of the C-

Table I. XRD Data for the C-EVA Composite Materials

C–EVA ratio (wt/wt)	2θ (°)	d-spacing (Å)	% Crystallinity
0/100	21.43 ± 0.0015	4.19 ± 0.0001	45.71 ± 0.0044
5/95	21.45 ± 0.0047	4.19 ± 0.0035	50.10 ± 0.0074
10/90	21.35 ± 0.0047	4.20 ± 0.0036	55.78 ± 0.0094
15/85	21.33 ± 0.0084	4.19 ± 0.0037	57.54 ± 0.0048
20/80	21.27 ± 0.0036	4.13 ± 0.0053	60.18 ± 0.0048
30/70	21.26 ± 0.0028	4.11 ± 0.0084	62.44 ± 0.0053

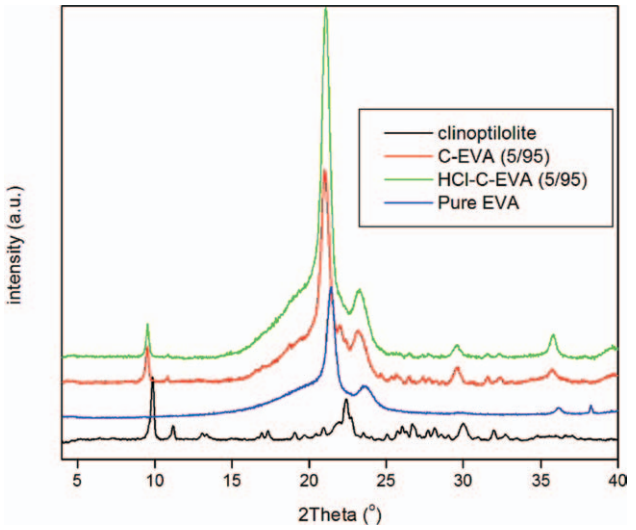

Figure 5. Effect of HCl treatment on XRD patterns. [Color figure can be viewed in the online issue, which is available at wileyonlinelibrary.com.]

EVA composites were modeled with the Pukanszky model, as shown in eq. (2). Pukanszky's model describes the effect of interfacial interaction and composition on the tensile yield or tensile strength of particulate-filled polymers.

$$\frac{\delta_{tc}}{\delta_{tm}} = \frac{1-\phi_f}{1+2.5\phi_f}\exp B_\sigma \phi_f \qquad (4)$$

In eq. (4), the interaction parameter B is related to the microscopic characteristics of the filler–matrix interface; ϕ_f is the fraction of the filler, while δ_{tc} and δ_{tm} denote the tensile yield (or strength) of the composite and matrix, respectively. The first term in eq. (4) relates to the decrease in effective load bearing cross-section, while the second one pertains to interfacial interaction. Parameter B in the second term characterizes the interaction between the filler and the matrix, and the higher the value of B, the better the compatibility.[22] In the present work, the values of B were found to be −0.1306 for C-EVA and −0.2126 for HCl-C-EVA composite. The negative B values are an indication of poor interfacial adhesion between the EVA polymer and the zeolite.

Table II. Tensile Test Results of the C-EVA Composite Films Filled with As Received Clinoptilolite

C–EVA ratio (% wt)	Young's modulus (MPa)	Tensile stress at break (MPa)	Elongation at break (%)
0/100	420.7	11.4	453.1
5/95	424.1	7.8	446.1
10/90	461.8	9.2	417.3
15/85	498. 1	8.5	369.8
20/80	537.6	7.9	353.7
30/70	447.9	6.2	344.5

Thermal Studies

TGA analysis of the HCl and as received EVA-C films showed very similar results. On average, degradation started at around 250°C, and terminated at about 540°C. The onset degradation temperature was, to a lesser extent, shifted to lower values with lower filler dosage, an indication that the C-EVA composite was more susceptible to thermal degradation at low zeolite content. The plain EVA, is however, more stable at lower temperatures as its degradation starts at a temperatures slightly above those of the composite films. The direct interface allows the inorganic domains to dissipate heat energy to the polymer matrix.[23,24]

Figure 6 shows thermograms of the plain EVA and those of as received and HCl-treated C-EVA films filled with 30 %weight of the zeolite. It can be observed that degradation of the plain polymer occurs in two steps—an initial step from 250 to 450°C which could be attributed to the removal of the acetyl group, and a final step from 450 to 540°C, which is the degradation of the main polymer chain. The filler looses mass continuously throughout the investigated temperature range although this mass is poorly visible in the composite samples, possibly due to its lower content. Although both samples were filled with 30% C, the weight losses at 540°C were 81.64% and 84.95% for the as received and HCl-C-EVA films, respectively. This inconsistency further confirms that the distribution of the filler within the polymer matrix was non-uniform. There is no significant shift to higher temperatures of the onset temperature with increasing filler content. However, the temperature of the maximum rate of weight loss (T_{max}) and the final decomposed temperature (FDT)[25] increased at 30% zeolite loading, compared with the pristine polymer. This is because the degradation of polymers is initiated with the formation of free radicals at weak bonds or chain ends, followed by their transfer to adjacent chains via inter-chain reaction. With an increased zeolite content therefore, the chain transfer reaction within the polymer is retarded, and as a result, the degradation process will be slowed hence decomposition will take place at higher temperatures.[26]

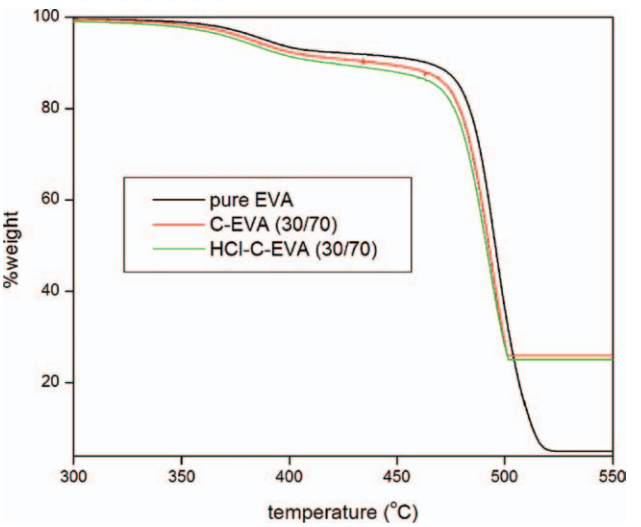

Figure 6. TGA curves of Plain EVA and 30 %wt of as received and HCl-treated zeolite-filled C-EVA composites. [Color figure can be viewed in the online issue, which is available at wileyonlinelibrary.com.]

CONCLUSIONS

As received and HCl-treated C-EVA composites were prepared via the melt-mixing technique, and the effects of zeolite loading and HCl activation of the filler on the thermal, mechanical, and structural properties of the composite films were investigated. The results show that addition of the C particles onto the polymer matrix leads to agglomeration of the particles, resulting in the formation of voids on the surface of the films. Consequently, the films become brittle at higher zeolite loading, resulting in reduced Young's modulus. Acid activation tends to alter the crystal structure of the zeolite, resulting in poor tensile properties of the HCl-treated zeolite-filled EVA films. Addition of the zeolite also increased the crystallinity of the structure, acting as a nucleating agent in the EVA crystallization. Thermal characterization studies showed that addition of the zeolites also retarded the onset degradation temperature of EVA. However, degradation temperatures including T_{max} and FDT were increased, suggesting improved thermal stability, due to reduced inter-chain mobility in the composite materials. The optimum conditions thus obtained in this study for the production of C-EVA composites are 15–20 %wt zeolite, without acid treatment.

ACKNOWLEDGMENTS

Funding for this project obtained from the DST/Mintek Nanotechnology Innovation Centre (NIC), National Research Foundation (NRF) and the University of Johannesburg (UJ) is greatly appreciated by the authors. Special thanks to Sasol Polymer Testing Centre for their assistance with the tensile tests.

REFERENCES

1. Pehlivan, H.; Balkose, D.; Ulku, S.; Tihminlioglu, F. *Compos. Sci. Technol.* **2005,** *65*, 2049.
2. Liu, T. B.; Burger C.; Chu, B. *Prog. Polym. Sci.* **2003,** *28*, 5.
3. Yang, K. K.; Wang, X. L.; Wang, Y. Z. *J. Ind. Eng. Chem.* **2007,** *13*, 485.
4. Supraka, S. R.; Pralay, M.; Masami, O. *Macromolecules* **2002,** *35*, 3104.
5. Gianelis, E. P. *Appl. Organomet. Chem.* **1998,** *12*, 675.
6. Ozmichi, F.; Balkose, D.; Ulku, S. J. *Appl. Polym. Sci.* **2001,** *82*, 2913.
7. Rozic, M.; Cerjan-Stefanovic, S.; Kurajika, S.; Vanica, V.; Hodzic, E. *Water Res.* **2000,** *34*, 3675.
8. Theng, B. K. G. The Chemistry of Clay-Organic Reactions; Wiley: New York, **1974.**
9. Motsa, M. M.; Mamba, B. B.; Thwala, J. M.; Msagati, T. A. *M. J. Coll. Int. Sci.* **2011,** *359*, 210.
10. Motsa, M. M.; Mamba, B. B.; Thwala, J. M.; Msagati, T. A. *J. Phys. Chem. Earth* **2011,** *36*, 1178.
11. Mthombo, T. S.; Mishra, A. K.; Mishra, S. B.; Mamba, B. B. *J. Appl. Polym. Sci.* **2011,** *121*, 3414.
12. Tsitsishvilli, G. V.; Andronikashvili, T. G.; Kirov, G. M.; Filizova, L. D. Natural Zeolites; Ellis Howood: Chichester; **1992.**
13. Madejova, J. *Vibtrat. Spectrosc.* **2003,** *3*, 1.
14. Kuronen, M.; Weller, M.; Townsend, R.; Harjula, R. *React. Funct. Polym.* **2006,** *66*, 1350.
15. Anirudhan, T. S.; Suchithra, P. S.; Rijith, S. *Eng. Aspects* **2008,** *326*, 147.
16. Ren, J.; Huang, Y.; Liu, Y.; Tang, X. *Polym. Test.* **2005,** *24*, 316.
17. Cullity, B. D.; Stock, S. R. Elements of X-ray Diffraction, 3rd ed.; Prentice-Hall: New Jersey, **2001.**
18. Al-Degs, Y.; Tutunji, M.; Baker, H. *Clay Miner.* **2003,** *38*, 501.
19. Inglezakis, V. J.; Grigoropoulou, H. J. *Hazard. Mater.* **2004,** *112*, 37.
20. Athanasiadis, K.; Helmreich, B. *Water Res.* **2005,** *39*, 1527.
21. Korkuna, O.; Leboda, R.; Skubiszewska-Zieba, J.; Vrublevs'ka, T.; Gun'ko, V. M.; Ryczkowski, J. *Micropor. Mesopor. Mater.* **2006,** *87*, 243.
22. Pukanszky, B.; Tudos, F. J. *Mater. Sci. Lett.* **1989,** *8*, 1040.
23. Park, S. J.; Kim, H. C. *J. Polym. Sci. Part B Polym. Phys.* **2001,** *39*, 121.
24. Dlamini, D. S.; Mishra, S. B.; Mishra, A. K.; Mamba, B. B. *J. Comp. Mater.* **2011,** *45*, 2211.
25. Dlamini, D. S.; Mishra, S. B.; Mishra, A. K.; Mamba, B. B. *J. Inorg. Organomet. Polym. Mater.* **2011,** *21*, 229.
26. Kulijanin, J.; Comor, M. I.; Djokovic, V.; Nedeljkovic, J. M. *Mater. Chem. Phys.* **2006,** *95*, 67.